Progress In Electromagnetics Research, Vol. 115, 131–146, 2011

SCATTERING ANALYSIS OF PERIODIC ARRAYS USING COMBINED CBF/P-FFT METHOD

K. Xiao, F. Zhao, S. L. Chai, and J. J. Mao

College of Electronic Science and Engineering
National University of Defense Technology
Changsha 410073, China

L. W. Li

Institute of Electromagnetics
University of Electronic Science and Technology of China
Chengdu 611731, China

Abstract—In this paper, an improved CBFM/p-FFT algorithm is presented, which can be applied to solve electromagnetic scattering problems of large-scale periodic composite metallic/dielectric arrays, even when the array has electrically small periodicity or separating distance. Using characteristic basis function method (CBFM), scattering characteristics of any inhomogeneous targets can be represented by special responses derived from a set of incident plane waves (PWs). In order to reserve the dominant scattering characteristics of the targets and remove the redundancy of the overfull responses, a singular value decomposition (SVD) procedure is applied, then, new series of basis functions are built based on the left singular vectors after SVD whose corresponding singular values beyond a predefined threshold. However, the algorithm of CBFM combined with method of moments (MoM) still requires a lot of memory and CPU resources to some large scale problems, so the precorrected-fast Fourier transform (p-FFT) method is applied based on the novel built basis functions, with which, the required memory and solve time for solution can be reduced in an extraordinary extent. For a near correction technique is applied to process the interactions between cells placed within a distance less than a predefined near-far field threshold, arrays with electrically small periodicity can be analyzed accurately. Moreover, the incomplete LU factorization with thresholding (ILUT) preconditioner is applied to improve the condition number of the combined algorithm, which improves the convergence speed greatly.

Received 6 February 2011, Accepted 15 March 2011, Scheduled 25 March 2011
Corresponding author: Ke Xiao (xiaoke_e@hotmail.com).

1. INTRODUCTION

Finite array problems, such as photonic crystals [1], metamaterials [2], phased antenna array [3], etc., have attracted considerable attention over the past one or two decades. To simplify the periodic array problem, some methods based on Floquent's theorem have been applied [4], where periodic Green's function was used [5], but the periodic structure is assumed to be infinitely periodical. In practical cases, periodic unit-cell dimensions are finite, when a more accurate solution should be obtained, all cells of the finite size must be considered to capture the mutual couplings and the fringe effects. Full-wave numerical approaches can be used to analyze such finite periodic structure problems, typical full-wave methods include the method of moments (MoM), the finite-difference time-domain method (FDTD), the finite element method (FEM), among which, one popular numerical method using MoM is based on the hybrid volume-surface integral equation (VSIE) [6, 7]. But to solve a dense matrix equation, the conventional MoM requires $O(N^3)$ computational complexity and $O(N^2)$ memory, which is inefficient for electrically large targets.

To render large problems manageable, hybrid methods are usually applied, where MoM is combined with asymptotic techniques [8, 9], then small objects with subtle changes can be treated with MoM, and the influence of big but smooth body is considered by asymptotic techniques such as GTD/UTD. However, to consider periodically composite structures, it is difficult for such hybrid method to provide accurate results. Another way to accelerate the calculation is to make use of novel basis functions, such as higher order basis function [10], some physically based entire-domain basis functions [11] and sub-entire-domain (SED) basis functions [12].

Since 1980s, fast solvers have been utilized to ease the requirement of memory and CPU time to an extent, such as conjugate gradient fast Fourier transform method (CG-FFT) [13], fast multipole algorithm (FMM) or multilevel fast multipole algorithm (MLFMA) [14, 15], adaptive integral method (AIM) [16] and precorrected-fast Fourier transform method (p-FFT) [17]. The p-FFT method is firstly proposed by Philips and White [18] to solve electrostatic integral equations and later extended to solve electromagnetic scattering or radiation problems [17, 19, 20]. When the volume integral equation (VIE) together with p-FFT is used, the complexity and memory are on the order of $O(N)$ and $O(N \log N)$ respectively, and for surface integral equation (SIE), the complexity and memory are on the order of $O(N^{1.5})$ and $O(N^{1.5} \log N)$ operations respectively.

Recently, the characteristic basis function method (CBFM)

has been introduced for an efficient analysis of electromagnetic problems [21, 22]. The characteristic basis functions (CBFs) are defined on macro domains, and derived by using the conventional triangular or tetrahedral discretization with RWG or SWG basis functions. The method leads to a much smaller matrix, and the mutual couplings and fringe effects can be considered rigorously. The CBFM has also been combined with some fast solvers [23–25], in [23], the CBFM has successfully been combined with FMM, and the algorithm was used to analyze scattering of microstrip antennas. In [24, 25], the CBFM algorithm was combined with fast solver p-FFT or AIM, and applied to analyze the scattering of dielectric finite periodic arrays, but the distance between cells of the described examples was set to $0.2\lambda_0$ which is beyond the distance of the near-far field threshold defined ordinarily, where near-correction of coupling between cells was not considered.

In this work, CBFM is combined with p-FFT to solve VSIE formulation, the scattering of composite metallic/dielectric arrays is analyzed by the so called CBFM/p-FFT algorithm. A set of incident plane waves (PWs) from adequate angles are used to excite unit-cell, then, a SVD procedure is applied to remove the redundant information of the responses, the left singular vectors, whose corresponding normalized singular values exceed a predefined threshold, are used to act as novel generated CBFs. Fast solver p-FFT is used to accelerate the matrix-vector multiplication based on the CBFs, so, the combined algorithm leads to a significant reduction in the requirements of memory and CPU time compared to the conventional CBFM or p-FFT algorithm. Besides, not only near-correction between inner CBFs in one cell is considered, near-correction between near CBFs in different cells is also considered, so periodic arrays with electrically small periodicity can be solved accurately using the algorithm. For iterative method is used for solution, ILUT preconditioner is applied to improve the condition number of the impedance matrix and speed up the convergence. Some numerical examples are presented to demonstrate the accuracy and capability of the combined method for solving periodic array problems.

2. FORMULATIONS AND EQUATIONS

Formulations including VSIE, CBFM and p-FFT are described in this section, the near-cell correction technique is introduced and combined to the CBFM/p-FFT algorithm.

2.1. VSIE Formulations

The basic idea of the VSIE approach is to use the volume equivalent principle to replace the unknown electric flux density in dielectric body with equivalent volume current density [26], the metal surface is replaced by surface currents using surface equivalent theorem [26], then, dyadic Green's function in free space can be used for the mixed problem. The scattering **E**-field is produced by $\mathbf{J}_c$ induced on the conducting surface and the equivalent volume polarization currents $\mathbf{J}_d$ as

$$\mathbf{E}^{\text{sca}} = i\omega\mu_b \left[\int_S \overline{\overline{G}}\left(\mathbf{r}, \mathbf{r}'\right) \mathbf{J}_c d\mathbf{r}' + \int_V \overline{\overline{G}}\left(\mathbf{r}, \mathbf{r}'\right) \mathbf{J}_d d\mathbf{r}' \right] \tag{1}$$

where the 3-D dyadic Green's function is expressed as

$$\overline{\overline{G}}\left(\mathbf{r}, \mathbf{r}'\right) = \left(\overline{\overline{I}} + \nabla\nabla/k_b^2\right) e^{ik_b|\mathbf{r}-\mathbf{r}'|} \Big/ \left(4\pi \left|\mathbf{r} - \mathbf{r}'\right|\right) \tag{2}$$

In which, k_b is the wavenumber in background media. Then, from the boundary condition on the conducting surface S and total electric field in the volume of dielectric body, two equations must be satisfied as follows:

$$\frac{\mathbf{D}\left(\mathbf{r}\right)}{\varepsilon\left(\mathbf{r}\right)} = \mathbf{E}^i\left(\mathbf{r}\right) + \mathbf{E}^s\left(\mathbf{r}\right) \quad \text{in } V_d \tag{3}$$

$$\mathbf{E}^i_{\tan} = -\mathbf{E}^s_{\tan} \quad \text{on } S_c \tag{4}$$

By following the procedure of MoM, the unknown electric flux density $\mathbf{J}_c$ and equivalent currents $\mathbf{J}_d$ are expanded using RWG and SWG respectively as follows

$$\mathbf{J}_S\left(\mathbf{r}\right) = \sum_{n=1}^{N_S} I_n^S \mathbf{f}_n^S\left(\mathbf{r}\right), \ \mathbf{r} \text{ on } S_c \tag{5}$$

$$\mathbf{D}_V\left(\mathbf{r}\right) = \sum_{n=1}^{N_V} I_n^V \mathbf{f}_n^V\left(\mathbf{r}\right), \ \mathbf{r} \text{ in } V_d \tag{6}$$

where N_S and N_V denote the number of unknowns of the conducting surfaces and dielectric volumes, respectively. The basis functions $\mathbf{f}_n^\gamma(\mathbf{r})$ used to expand the unknown currents are defined as

$$\mathbf{f}_n^\gamma(\mathbf{r}) = \begin{cases} \frac{\rho^\pm}{h_n^{\gamma\pm}}, & \mathbf{r} \text{ in } S_n^{\gamma\pm} \\ 0, & \text{otherwise} \end{cases} \tag{7}$$

where $S_n^{\gamma\pm}$ (with $\gamma = V$ or S) denotes the tetrahedron or triangle pair attached to the nth face or edge. The "$\pm$" designation of the

tetrahedron or triangle is determined by the choice of positive current reference direction for the nth face or common edge.

Galerkin method is used in the procedure of testing in the MoM, the method reduce the problem to the solution of N linear equations with N unknowns, and the matrix equation can be arrived as follow

$$\begin{bmatrix} \mathbf{Z}_{SS} & \mathbf{Z}_{SV} \\ \mathbf{Z}_{VS} & \mathbf{Z}_{VV} \end{bmatrix}_{N\times N} \begin{bmatrix} \mathbf{I}_S \\ \mathbf{I}_V \end{bmatrix}_N = \begin{bmatrix} \mathbf{V}_S \\ \mathbf{V}_V \end{bmatrix}_N \tag{8}$$

where $\mathbf{Z}_{\alpha\beta}$ ($\alpha,\ \beta = V$ or S) is the impedance matrix with the source basis function in β domain and the field basis function in α domain. $\mathbf{I}$ is the coefficient matrix of the electric flux in the dielectric volume and the currents on the conducting surface. $\mathbf{V}$ is the voltage matrix impressed by the exterior exciting such as plane wave input.

2.2. P-FFT Algorithm

The p-FFT algorithm is used to accelerate the calculation of matrix-vector products in (8), the basic idea of the algorithm is to consider the near- and far- zone interactions separately, in which, near-zone interactions within a predefined threshold are computed only once and stored [20], far-zone interactions are computed using FFT. The matrix-vector products can be approximated by following four-step procedure.

1) Projection: The currents and charges distributed on the original RWG/SWG meshes are projected onto auxiliary uniform grids by far-field matching at some given test points.

2) Convolution: The vector/scalar potentials at the uniform grid points can be computed efficiently using Fourier transform method.

3) Interpolation: Once the potentials on the auxiliary grid are calculated, the potentials on the original primary meshes can be obtained by locally interpolating from that of the uniform grids. The interpolation is actual the inverse procedure of projection.

4) Precorrection: For the above three steps are only accurate for far-field interactions, (2) should be utilized directly upon nearby elements, and the inaccurate contribution calculated by the far-field operator should be corrected accordingly.

So the p-FFT procedure can be expressed as

$$\mathbf{Z}^{p-FFT} = \mathbf{Q}^T\mathbf{H}\mathbf{W} + \mathbf{P} \tag{9}$$

where $\mathbf{W}$ represents the projection operator, $\mathbf{H}$ denotes the convolution operator, $\mathbf{Q}$ means the interpolation operator and $\mathbf{P}$ is the precorrection operator.

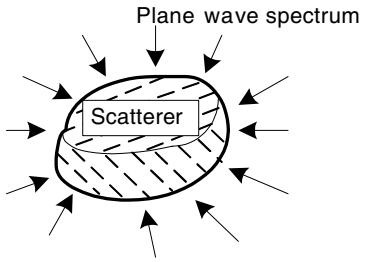

Figure 1. Plane wave spectrum on one cell.

2.3. Combined CBFM and P-FFT Algorithm

Referred to the physical optics (PO) method [21], the CBFs are generated from the currents induced by the Plane Wave Spectrum (PWS) on each block, and they are calculated using MoM combined with p-FFT before the coupling matrix is generated. For a scatterer as shown in Fig. 1, the number of unknowns due to the original irregular meshes (RWG or SWG) is denoted as N_S. A set of incident plane waves from $N^{PO} = N_\theta N_\phi$ angles are utilized as excitations of unit-cell, typically, the number of plane waves used to generate the CBFs should exceed the number of degrees of freedoms (DoFs) associate with the block [21]. The response matrix includes many redundant information, which can be eliminated by using singular value decomposition (SVD) as

$$\mathbf{J}^{CBFs} = \mathbf{LDR}^T \tag{10}$$

where the columns of $\mathbf{L}$ are called the left singular vectors of $\mathbf{J}$, and the columns of $\mathbf{R}$ are depicted as right singular vectors of $\mathbf{J}$, both of $\mathbf{L}$ and $\mathbf{R}$ are orthogonal matrix. In order to construct a new set of basis functions, only those with normalized singular values beyond a predefined threshold (typically chosen to be 10^{-3}) are retained. Thus, the left singular vectors in $\mathbf{L}$ related to the remained singular values in $\mathbf{D}$ are the generated CBFs after SVD and used to form the CBFs matrix expressed as $\mathbf{B}$. The number of CBFs is assumed to be K, which is always smaller than N^{PO}, then, under a certain exciting condition $\mathbf{V}$, the solution to the block can be denoted as

$$\mathbf{I} = \mathbf{BI}^C \tag{11}$$

where, $\mathbf{I}^C$ represents the unknown coefficients to the new constructed CBFs.

When a periodic array with M element cells is considered, the

matrix equation to the CBFs is written as [24, 25]

$$\begin{bmatrix} \mathbf{Z}_{11}^C & \mathbf{Z}_{12}^C & \cdots & \mathbf{Z}_{1M}^C \\ \mathbf{Z}_{21}^C & \mathbf{Z}_{22}^C & \cdots & \mathbf{Z}_{2M}^C \\ \vdots & \vdots & \ddots & \vdots \\ \mathbf{Z}_{M1}^C & \mathbf{Z}_{M2}^C & \cdots & \mathbf{Z}_{MM}^C \end{bmatrix} \begin{bmatrix} \mathbf{I}_1^C \\ \mathbf{I}_2^C \\ \vdots \\ \mathbf{I}_M^C \end{bmatrix} = \begin{bmatrix} \mathbf{V}_1^C \\ \mathbf{V}_2^C \\ \vdots \\ \mathbf{V}_M^C \end{bmatrix} \tag{12}$$

where $\mathbf{Z}_{mn}^C = \mathbf{B}_m^T \mathbf{Z}_{mn} \mathbf{B}_n$, $\mathbf{I}^C = \begin{bmatrix} \mathbf{I}_1^C & \mathbf{I}_2^C & \cdots & \mathbf{I}_M^C \end{bmatrix}^T$, $\mathbf{V}_m^C = \mathbf{B}_m^T \mathbf{V}_m$, $\mathbf{Z}_{mn}^C$ is the mutual coupling matrix of mth block and nth block, $\mathbf{I}^C$ are the unknown coefficients of CBFs to the entire problem, the right hand side of the matrix equation is the exciting vector.

The basic idea of p-FFT is used here to calculate the matrix-vector product of (12), and similar to (9), the procedure can be expressed as

$$\mathbf{Z}_{mn}^C = \mathbf{Q}_m^C \mathbf{H}^C \mathbf{W}_n^C + \mathbf{P}_{mn}^C \tag{13}$$

where, $\mathbf{W}_n^C = \mathbf{W}_n \mathbf{B}_n$, $\mathbf{H}^C = \mathbf{H}$, $\mathbf{Q}_m^C = \mathbf{B}_m{}^T \mathbf{Q}_m^T$, $\mathbf{P}_{mn}^C = \mathbf{B}_m^T \mathbf{P}_{mn} \mathbf{B}_n$, the operators are all constructed for CBFs, in which, $\mathbf{W}_n^C$ is the projection operator, $\mathbf{H}^C$ denotes the convolution operator, $\mathbf{Q}_m^C$ represents the interpolation operator and $\mathbf{P}_{mn}^C$ is the precorrection operator between block m and n. The precorrection procedure is only applied to calculate the interactions of near cells whose separation distance is within the predefined threshold.

To express the precorrection procedure more clearly, as shown in Fig. 2, there are two kinds of relations to consider the interactions between cell#1 and other cells, where, the legend "1" represents near-cell relation, and the interactions between nearby cells are poorly approximated by FFT procedure, so it is necessary to calculate the near-cell interactions directly and remove the inaccurate contribution of the far-cell calculation, while, "2" represents far-cell relation, which can be calculated by the FFT procedure accurately.

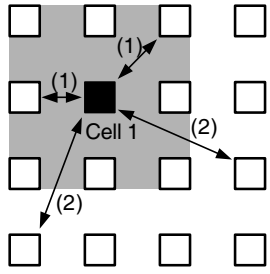

Figure 2. 2-D representation of the relationship between cells.

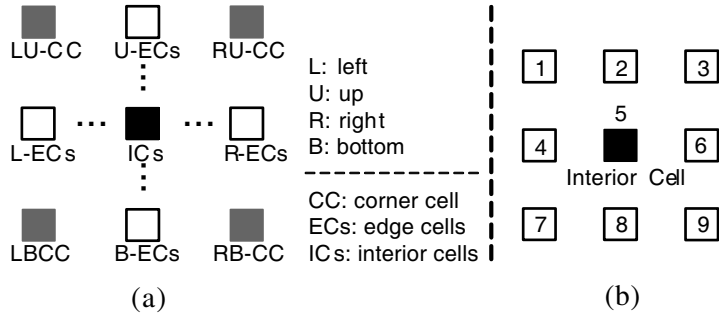

Figure 3. Near correction of cells: (a) Nine types of cells in the periodic structure, (b) interior cell representation.

To a 2-D periodic array, there are only nine kinds of cells as shown in Fig. 3(a), all the near-cell interactions can be included in Fig. 3(b), so only 9 types of near-cell interactions are needed to be calculated and stored.

2.4. Numerical Results

In this section, a number of examples will be shown. The first example considered is the calculation of radar cross section (RCS) of a conducting sphere coated with dielectric material. The radius of the inner sphere is $0.2\lambda_0$ ($\lambda_0 = 0.03\,\mathrm{m}$), the coated dielectric thickness is $0.024\lambda_0$, with a relative dielectric permittivity $\varepsilon_r = 2.2$. The coated ball is modeled by 1105 tetrahedral and 300 triangular cells. A plane wave is incident along the $+z$-axis direction, with incident electric field along the $+x$-axis direction. The bistatic RCS is calculated using MoM, and shown in Fig. 4(a), the exact solution using Mie series is also shown in the figure as reference. A good agreement is observed, except for a slight difference around $\theta = 0°$.

To make the retrieved CBFs involve the DOFs of the scatterer, we choose a PO number as 132, and solve the scattering problem again by the combined CBFM/pFFT algorithm, then, an equation is used to evaluate the relative error as follow

$$\Delta I_n = \frac{\left\| I_n^{MoM} - I_n^{CBFM/pFFT} \right\|_2}{\| I_n^{MoM} \|_2} \tag{14}$$

The error results for example I are plotted in Fig. 4(b), from which, the p-FFT algorithm has similar accuracy to the conventional MoM. The second example is the scattering analysis of a dielectric cubic covered by electrically infinite thin square conductor, as shown

in Fig. 5, the dielectric cubic ($\varepsilon_r = 2.2$) has a side length of $a = 0.38\lambda_0$. The composite metal-dielectric object is modeled by 1690 tetrahedral and 80 triangular cells. A plane wave is applied as the same as that in example I, the bistatic RCS obtained by the conventional MoM and the combined algorithm of this paper are presented in Fig. 6, and the error results are plotted in Fig. 5.

From the two examples discussed above, we can conclude that, PO number of 132 is enough for the calculation. The accuracy and efficiency of the MoM and combined CBFM/p-FFT algorithms are demonstrated.

In the third example, a 8×8 periodic array is considered, the structure of the element cell is shown in Fig. 5, but the dielectric cubic

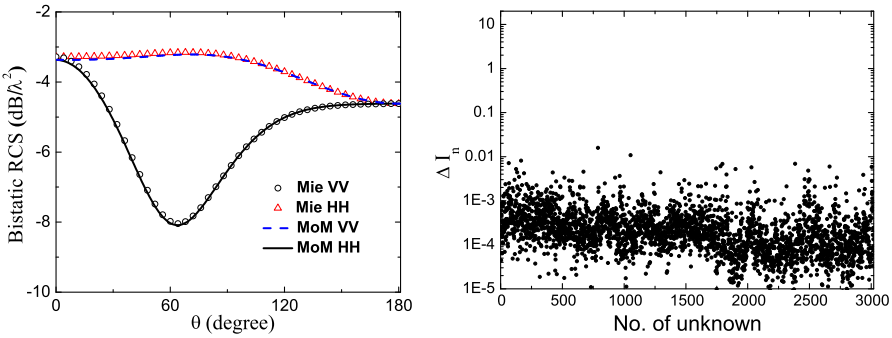

Figure 4. Bistatic RCS versus θ of the dielectric coated ball and calculated relative error.

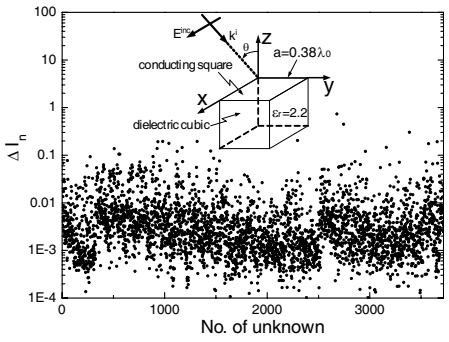

Figure 5. Model representation and calculated relative error of example II.

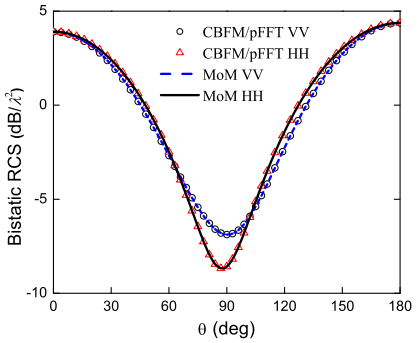

Figure 6. Bistatic RCS versus θ of the composite structure.

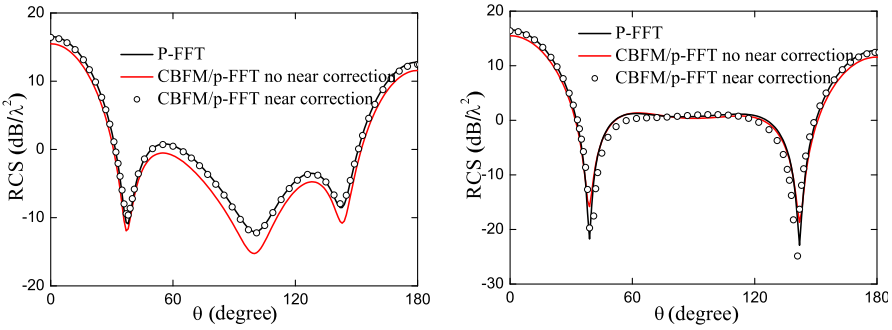

Figure 7. Bistatic RCS versus θ for the 8×8 array illuminated by an axially incident plane wave ($\theta = 0°$), whose electric field is along x-axis: (a) θ-polarization in x-z plane, (b) ϕ-polarization in y-z plane.

($\varepsilon_r = 2.2$) has a side length $a = 0.18\lambda_0$, and the periodicity is set as $0.2\lambda_0$ in x and y directions, 104 tetrahedral and 14 triangular cells are used to model one element structure. By using the algorithms of this paper, the bistatic RCS for θ-polarization component in x-z plane and ϕ-polarization component in y-z plane are calculated and depicted in Fig. 7. From the results, a good agreement is observed between the results of CBFM/p-FFT with near-cell correction procedure and the results of p-FFT algorithm, except slight differences exist around $\theta = 60°$ and $\theta = 120°$ in Fig. 7(b), while significant differences exist between the results of CBFM/p-FFT with no near-cell correction and p-FFT algorithm. The ILUT preconditioner [27] is applied in examples of this paper to improve the condition number for the combined algorithm, and the generalized minimum residual method (GMRES) is employed to solve the matrix equation for a faster convergence [28], the relative errors against the iterative times recorded are shown in Fig. 8, in which, the convergence is very poor in the case of not any preconditioner is used, while the convergence speed has been improved significantly after the preconditioner is applied.

Then, the periodicity of the array is changed to $0.4\lambda_0$, and the same normally incident plane wave is used for the calculation of RCS, the results are compared and shown in Fig. 9. For the space between nearby cells is $0.22\lambda_0$ which is larger than the predefined far-near field threshold, so similar results are obtained using the two approaches.

An oblique incidence case is also considered, a 10×10 periodic array whose periodicity is $0.2\lambda_0$ is constructed using element defined in example III. The incident angle is along the $\theta = 22°$ direction in y-z plane with the incident electric field still along the $+x$-axis

direction, the calculated results are compared to the conventional MoM and shown in Fig. 10. It is obvious that, the CBFM/p-FFT method approach with near-cell correction is more accurate than the approach with no considering the near-cell correction.

In the last example, a 6×6 coaxial line array is considered, as shown in Fig. 11. The element structure is a perfect conducting (PEC) cylinder coated with dielectric, the inner PEC cylinder has a length of $h = 0.5\lambda_0$ and a radius of $a = 0.03\lambda_0$, the coated dielectric ($\varepsilon_r = 2.2$) has an outer radius of $a = 0.07\lambda_0$, the periodicity of the array is set to $d = 0.2\lambda_0$. Each element is modeled by 289 tetrahedral and 78 triangular cells. A normally incident plane wave used before is applied here for RCS calculation, the results are depicted in Fig. 12. The relative errors against the iterative times recorded are shown in Fig. 13,

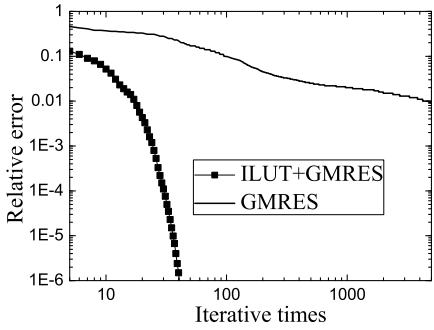

Figure 8. Relative error against the iterative times for the normal incidence case of example III.

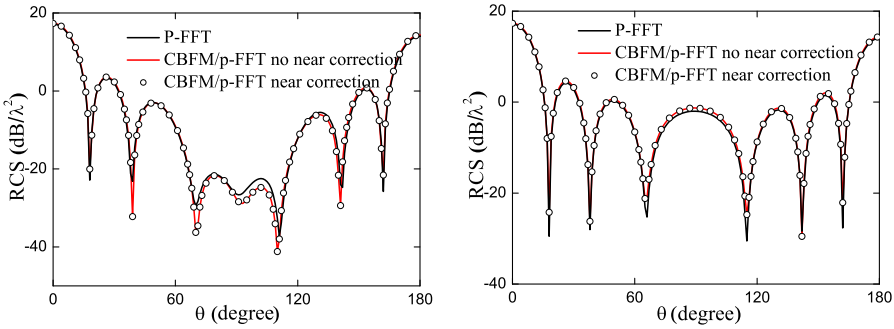

Figure 9. Bistatic RCS versus θ for the 8×8 array illuminated by the axially incident plane wave, the periodicity is $0.4\lambda_0$: (a) θ-polarization in x-z plane, (b) ϕ-polarization in y-z plane.

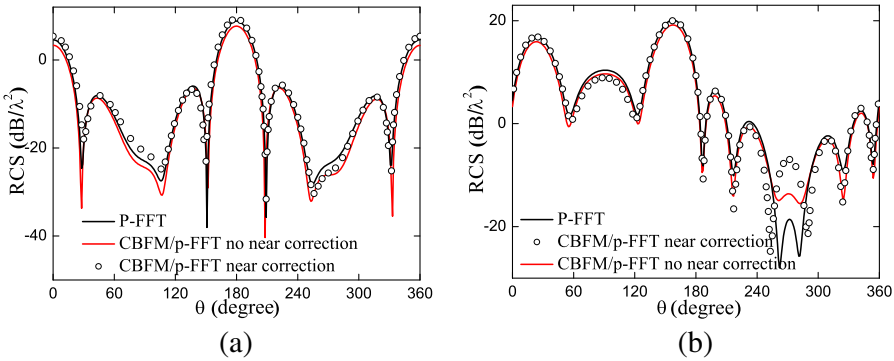

Figure 10. Oblique incidence case of the bistatic RCS versus θ for the 10×10 array, including the θ-polarization in x-z plane, and ϕ-polarization in y-z plane.

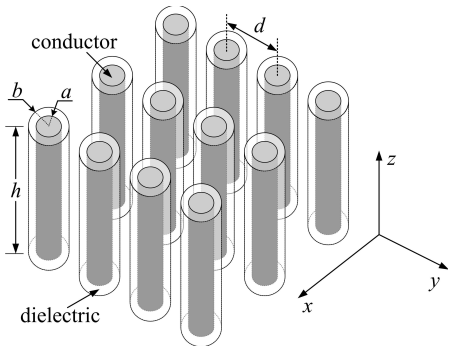

Figure 11. Geometry of a coaxial array.

from which, the convergence speed has also been improved significantly after the ILUT preconditioner is applied.

From the examples illustrated above, to solve an electrical small problem, the CPU time and memory requirement for retrieving CBFs take up most of the expends, while, to consider a large-scale problem, the expends for retrieving CBFs can be neglected. Exactly, if the periodic array has M cells, each cell has original meshed unknowns of N_s, and CBFs unknowns of K, then, for dielectric array problems, the memory requirement and computational complexity are of $O(MK)$ and $O(MK \cdot \log(MK))$, respectively, while, for simple metallic array problems, operations are of $O(MK)^{1.5}$ and $O(MK)^{1.5} \cdot \log(MK)$, respectively.

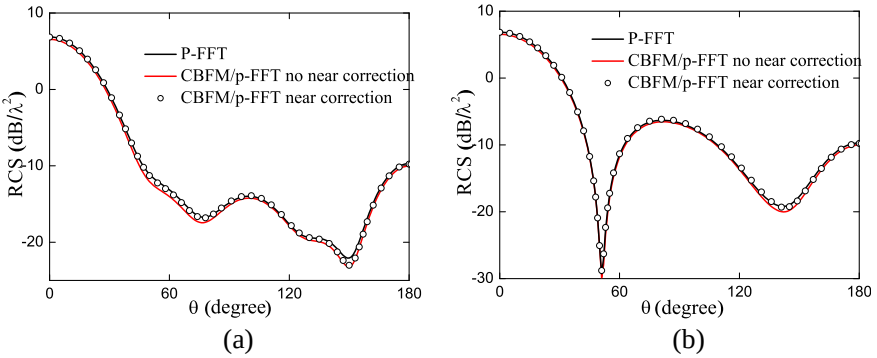

Figure 12. Bistatic RCS versus θ for the 6×6 coaxial array illuminated by the axially incident plane wave: (a) θ-polarization in x-z plane, (b) ϕ-polarization in y-z plane.

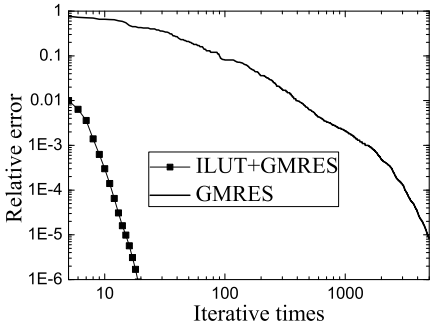

Figure 13. Relative error against the iterative times for the normal incidence case of example III.

3. CONCLUSION

In this paper, an improved CBFM/p-FFT algorithm to solve coupled volume-surface integral equations has been presented, near-cell correction technique is applied by considering interactions between nearby cells, electrically large composite (metal/dielectric) periodic arrays can be analyzed efficiently and accurately using the combined method even when the periodicity of the array is electrically small. By using SVD procedure, the unknowns reduction ratio defined by K/N_s is larger than 50 in examples illustrated in this paper, the memory and computational complexity requirements have been dramatically reduced compared to that of the conventional MoM. In the iterative solving procedure, we have used the preconditioner ILUT to accelerate the convenience. Several numerical examples about composite metal-

dielectric finite periodic arrays are demonstrated, good agreements between calculated results using the combined algorithm and using conventional MoM (or p-FFT) are obtained. It is ensured that the algorithm can be easily extended to radiation problems by adding the local source to the right hand side of (8) and (12), and the method can also be expanded to solve non-periodic structures, since it enables us to process different blocks to different CBFs. The detail will appear in a further publication.

ACKNOWLEDGMENT

The authors are grateful to Dr. Wei-Jiang Zhao, Dr. Li Hu from National University of Singapore and Dr. Zhong-Kuan Chen from National University of Defense Technology for their fruitful discussions and warm help.

REFERENCES

1. Joannopoulos, J. D., S. G. Johnson, J. N. Winn, and R. D. Meade, *Photonic Crystals: Molding the Flow of Light*, Princeton University Press, 2008.
2. Schurig, D., J. J. Mock, B. J. Justice, S. A. Cummer, J. B. Pendry, A. F. Starr, and D. R. Smith, "Metamaterial electromagnetic cloak at microwave frequencies," *Science*, Vol. 314, 977–980, 2006.
3. Buonanno, A., M. D'Urso, M. Cicolani, and S. Mosca, "Large phased arrays diagnostic via distributional approach," *Progress In Electromagnetics Research*, Vol. 92, 153–166, 2009.
4. Watanabe, K. and K. Yasumoto, "Accuracy improvement of the fourier series expansion method for Floquet-mode analysis of photonic crystal waveguides," *Progress In Electromagnetics Research*, Vol. 92, 209–222, 2009.
5. Bahadori, H., H. Alaeian, and R. Faraji-Dana, "Computation of periodic Green's functions in layered media using complex images technique," *Progress In Electromagnetics Research*, Vol. 112, 225–240, 2011.
6. Guo, J. L., J. Y. Li, and Q. Z. Liu, "Analysis of antenna array with arbitrarily shaped radomes using fast algorithm based on VSIE," *Journal of Electromagnetic Waves and Applications*, Vol. 20, No. 10, 1399–1410, 2006.
7. Shi, Y., X. Luan, J. Qin, C. J. Lv, and C. H. Liang, "Multilevel Green's function interpolation method solution of volume-surface integral equation for mixed conducting/bi-isotropic objects," *Progress In Electromagnetics Research*, Vol. 107, 239–252, 2010.

8. Thiele, G. A. and T. H. Newhouse, "A hybrid technique for combining moment methods with the geometrical theory of diffraction," *IEEE Trans. Antennas Propagat.*, Vol. 23, No. 1, 62–69, Jan. 1975.
9. Lertwiriyaprapa, T., P. H. Pathak, and J. L. Volakis, "An approximate UTD ray solution for the radiation and scattering by antennas near a junction between two different thin planar material slab on ground plane," *Progress In Electromagnetics Research*, Vol. 102, 227–248, 2010.
10. Eibert, T. F., Ismatullah, E. Kaliyaperumal, and C. H. Schmidt, "Inverse equivalent surface current method with hierarchical higher order basis functions, full probe correction and multi-level fast multipole acceleration," *Progress In Electromagnetics Research*, Vol. 106, 377–394, 2010.
11. Suter, E. and J. Mosig, "A subdomain multilevel approach for the MoM analysis of large planar antennas," *Microwave Opt. Technol. Lett.*, Vol. 26, No. 4, 270–277, Aug. 2000.
12. Du, P., B. Z. Wang, H. Li, and G. Zheng, "Scattering analysis of large-scale periodic structures using the sub-entire domain basis function method and characteristic function method," *Journal of Electromagnetic Waves and Applications*, Vol. 21, No. 14, 2085–2094, 2007.
13. Gan, H. and W. C. Chew, "Discrete BCG-FFT algorithm for solving 3D inhomogeneous scatterer problems," *Journal of Electromagnetic Waves and Applications*, Vol. 9, No. 10, 1339–1357, 1995.
14. Brandfass, M. and W. C. Chew, "A multilevel fast multipole based approach for efficient reconstruction of perfectly conducting scatterers," *Journal of Electromagnetic Waves and Applications*, Vol. 15, No. 1, 81–106, 2001.
15. Taboada, J. M., M. G. Araújo, J. M. Bértolo, L. Landesa, F. Obelleiro, and J. L. Rodriguez, "MLFMA-FFT parallel algorithm for the solution of large-scale problems in electromagnetics," *Progress In Electromagnetics Research*, Vol. 105, 15–30, 2010.
16. Ling, F., C. F. Wang, and J. M. Jin, "Application of adaptive integral method to scattering and radiation analysis of arbitrarily shaped planar structures," *Journal of Electromagnetic Waves and Applications*, Vol. 12, No. 8, 1021–1037, 1998.
17. Nie, X. C., L. W. Li, and N. Yuan, "Precorrected-FFT algorithm for solving combined field integral equations in electromagnetic scattering," *Journal of Electromagnetic Waves and Applications*, Vol. 16, No. 8, 1171–1187, 2002.

18. Phillips, J. R. and J. K. White, "A precorrected-FFT method for electrostatic analysis of complicated 3-D structures," *IEEE Trans. Computer-aided Design of Integrated Circuits and Systems*, Vol. 16, No. 10, 1059–1072, Oct. 1997.
19. Yuan, N., T. S. Yeo, X. C. Nie, L. W. Li, and Y. B. Gan, "Analysis of scattering from composite conducting and dielectric targets using the precorrected-FFT algorithm," *Journal of Electromagnetic Waves and Applications*, Vol. 17, No. 3, 499–515, 2003.
20. Yuan, N., X. C. Nie, Y. B. Gan, T. S. Yeo, and L. W. Li, "Accurate analysis of conformal antenna arrays with finite and curved frequency selective surfaces," *Journal of Electromagnetic Waves and Applications*, Vol. 21, No. 13, 1745–1760, 2007.
21. Lucente, E., A. Monorchio, and R. Mittra, "An iteration-free MoM approach based on excitation independent characteristic basis functions for solving large multiscale electromagnetic scattering problems," *IEEE Trans. Antennas Propagat.*, Vol. 56, No. 4, 999–1007, Apr. 2008.
22. Laviada, J., R. G. Ayestarán, M. R. Pino, F. Las-Heras Andrés and R. Mittra, "Synthesis of phased arrays in complex environments with the multilevel characteristic basis function method," *Progress In Electromagnetics Research*, Vol. 92, 347–360, 2009.
23. Wan, J. X., and C. H. Liang, "A fast analysis of scattering from microstrip antennas over a wide band," *Progress In Electromagnetics Research*, Vol. 50, 187–208, 2005.
24. Hu, L. and L. W. Li, "CBFM-based p-FFT method: A new algorithm for solving large-scale finite periodic arrays scattering problems," *APMC: Asia Pacific Microwave Conference*, 88–91, 2009.
25. Hu, L., L. W. Li, and R. Mittra, "Electromagnetic scattering by finite periodic arrays using the characteristic basis function and adaptive integral methods," *IEEE Trans. Antennas Propagat.*, Vol. 58, No. 9, 3086–3090, Sep. 2010.
26. Balanis, C. A., *Advanced Engineering Electromagnetics*, Wiley-Interscience, New York, 1989.
27. Saad, Y., "A dual threshold incomplete LU preconditioner," *Numerical and Linear Algebra and its Applications*, Vol. 1, No. 4, 387–402, 1994.
28. Saad, Y., "GMRES: A generalized minimal residual algorithm for solving nonsymmetric linear systems," *SIME J. Sci. Stat. Comput.*, Vol. 7, No. 3, 856–869, 1986.